THEORETICA CHIMICA ACTA

Theoret. Chim. Acta (Berl.) 67, 391-407 (1985)

Extension of a simplified method for molecular correlation energy calculations to molecules containing third row atoms II. Application to HCl, HCl^+, ClO and NCl molecules

Jacques Lievin and Jean-Yves Metz*

Laboratoire de Chimie Physique Moléculaire, Faculté des Sciences, CP.160, Université Libre de Bruxelles, B-1050 Bruxelles, Belgium

A simplified method for molecular correlation energy calculations developed in I is applied to the determination of the potential curves of some diatomic chlorinated molecules $HCl(^1\Sigma^+)$, $HCl^+(^2\Pi)$, $ClO(^2\Pi)$ and $NCl(X^3\Sigma^-, a^1\Delta, b^1\Sigma^+)$. Dissociation energies, vibrational frequencies and equilibrium internuclear distances are derived from these curves. The ionisation potential (I_p) of HCl, the proton affinity (PA) of Cl, and the term energies of the excited states of the NCl radical are also calculated. It is shown that the results are very sensitive to correlation effects and that the correlated results converge to the corresponding experimental values within 10% for PA, D_e, T_e and ω_e, 2% for R_e and 0.3% for I_p. This agreement allows us to predict the following lower limits for the dissociation energies of the NCl radical: 2.14, 3.28 and 2.47 eV respectively for the $X^3\Sigma^-$, $a^1\Delta$ and $b^1\Sigma^+$ states. Results on HF and HF^+ are also discussed and compared with those obtained for HCl and HCl^+.

Key words: *Ab initio* calculation—correlation energy—hydrogen chloride—hydrogen chloride ion—chlorine monoxide—nitrogen chloride—hydrogen fluoride—hydrogen fluoride ion

1. Introduction

In the first paper of this series (referred to as I), we have proposed an extension to molecules containing third row atoms of a simplified method for the calculation

* Boursier IRSIA

of molecular correlation energies. The chlorine atom was chosen to test the methodology and the required numerical parameters (parameters for the $3d$ polarization and correlation orbitals, and semi-empirical atomic data) were derived for this atom.

In this work, we apply the method to some simple chlorinated molecules like HCl, HCl^+, ClO and NCl and discuss the accuracy of the results obtained for these systems for different types of calculated properties: equilibrium geometries, vibrational frequencies, dissociation energies, term energies, ionisation potentials and proton affinities. The results will be analysed in terms of the progressive inclusion of the correlation energy by considering the different contributions to the energy partition, which is the basic idea of the method.

Test calculations will be first carried out on HCl, HCl^+ and ClO for which numerous experimental data are available, moreover this choice will allow interesting comparisons to be made between neutral and ionic species. Finally, molecular parameters will be calculated for the three lowest states of NCl which is a free radical for which relatively little information is available either experimentally or theoretically so that valuable predictions may be made.

2. Calculations

The results presented in the next sections will be discussed on the basis of the three terms that define the energy partition:

$$E \simeq E_0 + E^{\mathrm{I}}_{\mathrm{CORR}} + E_{\mathrm{E}}. \tag{1}$$

Let us recall (see I) that:

i) E_0 refers to the energy of the zeroth order wavefunction Ψ_0 and is obtained by an MCSCF calculation performed with an extended polarized basis set;

ii) $E^{\mathrm{I}}_{\mathrm{CORR}}$ is the internal correlation energy determined by a complete CI calculation (mono and biexcitations with respect to Ψ_0) performed with a minimal basis set augmented by a $3d$ correlation orbital on the chlorine atom;

iii) E_{E} has been defined as the error energy regrouping the non-internal correlation energy and the relativistic energy contributions. It is obtained by an "atoms-in-molecule" decomposition of the zeroth order wavefunction calculated with the minimal basis set used in ii).

Calculated values of these energy components obtained for the NCl radical are given in Table 1. The potential curves were derived from these results at the three following levels of calculation, in order to discuss the effect of a progressive inclusion of the correlation energy: E_0, $E_0 + E^{\mathrm{I}}_{\mathrm{CORR}}$ and $E_0 + E^{\mathrm{I}}_{\mathrm{CORR}} + E_{\mathrm{E}}$. On the basis of previous works [1, 2], we can make the following general comments concerning the qualitative behavior of the potential curves at the three different levels of calculation. First, we expect in the general case a flattening of the potential curves at the zeroth-order wavefunction level, with too large R_e values and too small ω_e and D_e values. This observation is a direct consequence of the

Table 1. Energy contributions for NCl[a] and its dissociation products (a.u.)

System	E_0	E^I_{CORR}	E_E	$E^I_{CORR}+E_E$
$N(^4S)$	−9.6296	0.	−0.213	−0.213
$N(^2D)$	−9.5229	0.	−0.230	−0.230
$Cl(^2P)$	−14.6562	−0.0962	−1.802	−1.898
$NCl(^3\Sigma^-)$	−24.3279	−0.1192	−2.029	−2.148
$NCl(^1\Delta)$	−24.2600	−0.1272	−2.041	−2.168
$NCl(^1\Sigma^+)$	−24.2099	−0.1543	−2.034	−2.188

[a] Values for NCl are given at the corresponding equilibrium geometries

unbalanced wavefunction that is used: Ψ_0 gives rise to an underestimated dissociation energy corresponding approximately to the energy difference between the molecule at its equilibrium geometry and the Wigner-Witmer products, both calculated at the SCF level, and this difference is of course too small because the correlation energy contents of the molecule is bigger than that of the products. The effect of including first the internal and then the non-internal correlation energy is to improve successively the energy balance between the regions of the potential curves respectively at short and large internuclear distances, so that the total energy results ($E_0+E^I_{CORR}+E_E$) converge to the corresponding experimental results. These qualitative observations will appear systematically in the results presented in the next section so that later on we will restrict ourselves to particular comments when necessary.

The parameters of the potential curves (R_e, ω_e and $E(R_e)$) have been determined from polynomial fittings of degrees 4 to 6. $E(R_e)$ and $E(R\to\infty)$ values have been used to obtain the energy differences such as D_e, T_e....

The results of the molecular parameters calculated at the three levels of energy partition are presented and compared to the corresponding experimental values in Tables 2 to 4 for HCl and HCl^+, 7 for ClO and 8 for NCl.

Table 2. Molecular parameters for $HCl(^1\Sigma^+)$

Level of approximation	Basis set[a]	R_e (a.u.)	ω_e (cm^{-1})	D_e (eV)
E_0	DZP	2.44	2982	3.89
$E_0+E^I_{CORR}$	DZP/MB5	2.43	2989	4.00
$E_0+E^I_{CORR}+E_E$	DZP/MB5	2.40	3083	4.63
Exp.[b]		2.41	2991	4.62
SCEP/CEPA[c]	$[14s11p3d1f/7s2p1d_\sigma]$	2.42	2987	—
PNO/CEPA[c]	$[14s11p3d1f/7s2p1d_\sigma]$	2.42	2977	—
POL/CI[d]	$[4s4p1d/2s1p]$	2.42	—	4.62

[a] See comments in the text.
[b] Ref. [3]; $D_e=D_0+\omega_e/2$.
[c] Gaussian basis set, Ref. [7].
[d] Gaussian basis set, Ref. [8]

Table 3. Molecular parameters of $HCl^+(^2\Pi)$

Level of approximation	Basis set[c]	R_e (a.u.)	ω_e (cm^{-1})	D_e (eV)
E_0	DZP	2.49	2818	4.10
$E_0+E^I_{CORR}$	DZP/MB5(1)	2.48	2858	4.37
	DZP/MB5(2)	2.48	2862	4.27
$E_0+E^I_{CORR}+E_E$	DZP/MB5(2)	2.47	2899	4.97
Exp.		2.48[a]	2674[a]	4.82[a]
				4.86[b]
CEPA[d]	[4s4p2d1f/4s2p1d]	2.49	2688	4.77
PNO-CI[d]	[4s4p2d1f/4s2p1d]	2.48	2737	

[a] Ref. [3]; $D_e = D_0 + \omega_e/2$.
[b] Ref. [4].
[c] See comments in the text.
[d] Gaussian basis set, Ref. [9]

Table 4. Ionisation potential for HCl and proton affinity for Cl

Level of approximation	Basis set[a]	*PA* (eV)	$I_p^{(1)}$ (eV)[a]	$I_p^{(2)}$ (eV)[a]	$I_p^{(3)}$ (eV)[a]
E_0	DZP	5.08	12.20	11.77	11.77
$E_0+E^I_{CORR}$	DZP/MB5(*a*)	5.22	12.17	12.04	11.82
	DZP/MB5(*b*)	5.43			
$E_0+E^I_{CORR}+E_E$	DZP/MB5(*a*)	4.97	13.04	13.00	12.78
	DZP/MB5(*b*)	5.19			
Exp.		5.46[b]		12.748 ± 0.005[c]	
CEPA[d]	[4s4p2d1f/4s2p1d]	5.36		12.49	

[a] See comments in the text.
[b] Estimated as $D_e(HCl^+)+I_p(H)-I_p(Cl)$.
[c] Ref. [5].
[d] Gaussian basis set, Ref. [9]

2. The HCl and HCl^+ molecules

2.1. Zeroth-order wavefunction for HCl

Following the Wigner-Witmer rules, the ground $^1\Sigma^+$ state of the HCl molecule dissociates according to:

$$HCl(X^1\Sigma^+) \rightarrow H(^2S)+Cl(^2P). \tag{2}$$

The zeroth order wavefunction describing this process is readily written as[1]:

$$\Psi_0(HCl; X^1\Sigma^+) = 1\sigma^2(c_1 2\sigma^2 + c_2 2\sigma 3\sigma + c_3 3\sigma^2)1\pi^4. \tag{3}$$

[1] Throughout this paper, only the valence orbitals will be considered and labelled from 1 to *n*

A further investigation of the wavefunction shows that the following rotation between the 2σ and 3σ orbitals:

$$\begin{pmatrix} 2\sigma \\ 3\sigma \end{pmatrix} = \begin{pmatrix} \cos\Theta & \sin\Theta \\ -\sin\Theta & \cos\Theta \end{pmatrix} \begin{pmatrix} 2\sigma' \\ 3\sigma' \end{pmatrix} \tag{4}$$

allows us to rewrite the second SAAP of (3) as

$$\begin{aligned} 1\sigma^2 2\sigma 3\sigma\{^1\Sigma^+\}1\pi^4 &= \frac{1}{\sqrt{2}} 1\sigma^2(2\sigma\overline{3\sigma} - \overline{2\sigma}3\sigma)1\pi^4 \\ &= \frac{\sin 2\Theta}{\sqrt{2}} 1\sigma^2(3\sigma'^2 - 2\sigma'^2)1\pi^4 \\ &\quad + \cos 2\Theta\, 1\sigma^2 2\sigma' 3\sigma'\{^1\Sigma^+\}1\pi^4 \end{aligned} \tag{5}$$

where { } indicates the intermediate coupling of the 2σ and 3σ orbitals. A particular choice of $\Theta = \pi/4$ cancels the open shell term so that an expression for Ψ_0 equivalent to (3) is:

$$\Psi_0'(\mathrm{HCl};\, ^1\Sigma^+) = 1\sigma^2(c_1' 2\sigma'^2 + c_2' 3\sigma'^2)1\pi^4. \tag{6}$$

Such a reduction of the zeroth-order wavefunction obviously reduces the calculation times for the three parts of the energy (see (1)). Unfortunately, as will be shown below, it only applies to open-shell SAAP's with singlet coupling.

2.2. Molecular parameters for HCl

An examination of Table 2 prompts the following comments concerning the calculated vibrational frequency. The introduction of the error energy modifies the agreement with the experimental value found at the $E_0 + \tilde{\varepsilon}^{\mathrm{I}}_{\mathrm{CORR}}$ level only slightly. In fact, we generally observe a somewhat erratic dependence of ω_e with E_{E} for all the systems studied here. Finally, the total energy results ($E_0 + E^{\mathrm{I}}_{\mathrm{CORR}} + E_{\mathrm{E}}$) are in very nice agreement with the corresponding experimental values with discrepancies of only 0.4%, 3% and 0.2% for R_e, ω_e and D_e respectively.

2.3. Zeroth-order wavefunction for HCl^+

The zeroth-order wavefunction describing the process:

$$\mathrm{HCl}^+(X^2\Pi) \rightarrow \mathrm{H}(^2S) + \mathrm{Cl}^+(^3P) \tag{7}$$

is very similar to (2), i.e.:

$$\Psi_0(\mathrm{HCl}^+;\, X^2\Pi) = 1\sigma^2(c_1 2\sigma^2 + c_2 2\sigma 3\sigma + c_3 3\sigma^2)1\pi^3. \tag{8}$$

Making the rotation (4) between the 2σ and 3σ oribitals, the second SAAP of (8):

$$1\sigma^2 2\sigma 3\sigma 1\pi^3(^2\Pi) = \mathrm{A}\; 1\sigma^2 2\sigma 3\sigma\{^1\Sigma^+\}1\pi^3(^2\Pi) + \mathrm{B}\; 1\sigma^2 2\sigma 3\sigma\{^3\Sigma^+\}1\pi^3(^2\Pi)$$

where { } and ( ) indicate the intermediate and final couplings respectively, can

be rewritten as

$$\frac{A\sin 2\Theta}{\sqrt{2}}1\sigma^2(3\sigma'^2-2\sigma'^2)1\pi^3+A\cos 2\Theta 1\sigma^2 2\sigma' 3\sigma'\{^1\Sigma^+\}1\pi^3$$

$$+B\,1\sigma^2 2\sigma' 3\sigma'\{^3\Sigma^+\}1\pi^3. \tag{9}$$

Since there is no Θ dependance for the triplet recoupling term, it cannot be made to disappear so that a diagonal form similar to (6) does not exist for (8).

2.4. Molecular parameters for HCl^+

Table 3 shows that in this case, the equilibrium internuclear distance is already nicely described at the MC_0 level and is very slightly modified only by the inclusion of the correlation energy. The vibrational frequency increases with the inclusion of the correlation energy which is a qualitatively correct result. However, in this case the value calculated at the MC_0 level is already too high.

The comparison between MB5(1) and MB5(2) shows that the basis set effect on the internal correlation energy due to the optimization of the $3d$ correlation orbital on Cl or Cl^+ respectively (see I section 5.2.2) is only significant for D_e which is improved by an amount of 0.1 eV. Finally, the agreement between the experimental and the calculated parameters are 0.6%, 8.5% and 3% for R_e, ω_e and D_e respectively.

2.5. Proton affinity of the Chlorine atom

The proton affinity of the chlorine atom in its ground ^2P state is defined as the energy difference associated to the process:

$$Cl(^2P)+H^+(^1S)\rightarrow HCl^+(X^2\Pi). \tag{10}$$

The corresponding zeroth-order wavefunction is the SCF wavefunction of HCl^+ in its ground $^2\Pi$ state because the molecular orbitals of this wavefunction asymptotically correlate to those of Cl and H^+:

$$\Psi_0=1\sigma^2 2\sigma^2 1\pi^3. \tag{11}$$

On the basis of the results of Table 4, we can discuss the consequences of the inclusion of the correlation energy on the calculated proton affinity (PA).

First we note that the choice of a unique $3d$ correlation orbital cannot be optimal in this case. Indeed we have discussed in I, the non-transferability of the $3d$ correlation orbital from neutral systems like Cl and HCl to ionic ones like Cl^+ and HCl^+ and inversely. In the case of the dissociation of HCl^+ into $H+Cl^+$, discussed in the previous section, the use of the $3d$ orbital optimized on Cl^+ does not unbalance the correlation energy along the dissociation curve because no drastic charge transfer occurs on the Cl atom. On the contrary, in the case of process (10), the protonation induces a transfer of electrons from chlorine to hydrogen, so that the use of the $3d$ orbital optimized on Cl to calculate both HCl^+ and $Cl+H^+$ will underestimate the corresponding proton affinity value.

The opposite effect is of course expected if we use the $3d$ function optimized on Cl^+. In order to estimate the magnitude of this effect, in Table 4 we compare the results of two separate calculations. In the first one (MB5(a)), both HCl^+ and $H^+ + Cl$ are calculated with the $3d$ orbital optimized on Cl, and in the second one (MB5(b)), each partner is calculated with its optimal $3d$ orbital, i.e. the orbital optimized on Cl^+ for HCl^+ and on Cl for $H^+ + Cl$. As can be seen, the basis effect is 0.2 eV, which is certainly not negligible. For such energy differences calculations, two distinct correlation orbitals can easily be optimized, but similar complete optimization are of course much more tedious for potential energy hypersurfaces calculations.

The consequence of the inclusion of the internal correlation energy is to increase the proton affinity, HCl^+ having more internal correlation energy than $H^+ + Cl$. The effect of the inclusion of the error energy is to decrease the proton affinity, due to the fact that the "atoms-in-molecule" structures occurring in HCl^+ giving rise to ionic combinations other than that of $Cl + H^+$ are mainly $H + Cl^+$ and $H^- + Cl^{++}$ which have both less error energy than $Cl + H^+$ itself. Finally, the agreement between the calculated proton affinity and the one obtained from the cycle: $D_e^{exp}(HCl^+) + I_p^{exp}(H) - I_p^{exp}(Cl)$ is not too bad, the former being too small by an amount of 5%.

2.6. Ionisation potential of HCl

The ionisation potential of HCl is calculated by separate calculations on HCl and HCl^+ and hence we need two zeroth-order wavefunctions. For HCl, we chose the zeroth-order wavefunction (6) corresponding to the dissociation process of this molecule and for HCl^+ we chose the zeroth-order wavefunction (11) and (8) corresponding to the SCF and to the dissociative wavefunction respectively. The corresponding ionisation potentials calculated using the $3d$ polarisation orbital optimized on Cl are presented in Table 5 and are labelled $I_p^{(1)}$ and $I_p^{(2)}$. At the E_0 level, $I_p^{(1)}$ is greater than $I_p^{(2)}$ because the zeroth-order wavefunctions used for HCl and HCl^+ are not equivalent. In fact the multiconfiguration used to calculate HCl includes a part of the internal correlation energy while the SCF configuration used for HCl^+ does not. The incorporation of the remaining correlation energy reduces this difference which finally almost cancels. This result shows that the $MC_n(ext)/\Delta CI(min) + E_E$ procedure used to calculate the correlation energy is to a good approximation independent of n as already pointed out previously [1]. Finally, $I_p^{(3)}$ is calculated using the same zeroth-order wavefunction for HCl^+ as $I_p^{(2)}$ but with an internal correlation energy of HCl^+ calculated using the $3d$ correlation orbital optimized on Cl^+. The importance of this specific optimization already pointed out in I leads to a smaller value for the ionisation potential that agrees very well (0.25%) with the corresponding experimental result.

2.7. Comparison between second- and third-row hydrides

In this section we present results on HF and HF^+ (see Tables 5 and 6) in order to compare the level of accuracy of our results for similar second- and third-row atom systems. A one primitive $3d$ polarization orbital has been optimized for

Table 5. Molecular parameters of HF($^1\Sigma^+$)

Level of approximation	Basis set[a]	R_e (a.u.)	ω_e (cm^{-1})	D_e (eV)	I_p (eV)
$E_0+E^1_{CORR}+E_E$	DZP/MB5	1.70	4030	5.83	15.64
Exp.		1.73[b]	4138[b]	6.12[b]	16.044[c]
MCSCF[d]	[5s3p2d/3s1p]	1.737	4102	—	—
CEPA[e]	[4s4p2d1f/4s2p1d]	1.733	4169	5.83	—
MRD-CI[f]	[6s6p1d/3s1p]	1.745	4148	5.98	—
CEPA[g]	[4s4p2d1f/4s2p1d]	—	—	—	15.74

[a] See comments in the text.
[b] Ref. [3]; $D_e = D_0 + \omega_e/2$.
[c] Ref. [9].
[d] Gaussian basis set, Ref. [11].
[e] Gaussian basis set, Ref. [12].
[f] Gaussian basis set including Rydberg orbitals, Ref. [13].
[g] Gaussian basis set, Ref. [9]

Table 6. Molecular parameters of HF$^+$($^2\Pi$)

Level of approximation	Basis set[a]	R_e (a.u.)	ω_e (cm^{-1})	D_e (eV)
$E_0+E^1_{CORR}+E_E$	DZP/MB5	1.88	3111	3.68
Exp.[b]		1.89	3090	3.61
CEPA[c]	[4s4p2d1f/4s2p1d]	1.89	3116	3.64

[a] See comments in the text.
[b] Ref. [9], $D_e = D_0 + \omega_e/2$.
[c] Gaussian basis set, Ref. [9]

the fluorine atom on the HF molecule. The optimized value of the Gaussian exponent is 1.1. HF$^+$ calculations have been performed with the same polarization function (see *I* section 5.1 for a discussion on the transferability of such orbitals). No 3*d* correlation orbital was introduced in the calculation because the near-degeneracy of the fluorine atom takes place in the $n = 2$ shell.

The results presented in Tables 5 and 6 are found to be in good agreement with the corresponding experimental and other calculated results. This agreement is quite similar to that observed in the previous sections for HCl and HCl$^+$. This comparison reinforces our confidence in the semi-empirical procedure which seems to constitute a balanced treatment of second- and third-row atoms.

3. The ClO radical

3.1. Zeroth-order wavefunction for ClO

The ground $^2\Pi$ state of the ClO radical, dissociates according to the Wigner-Witmer rules to the atomic products in their ground states:

$$ClO(X^2\Pi) \rightarrow Cl(^2P) + O(^3P). \tag{12}$$

Table 7. Molecular parameters of ClO ($^2\Pi$)

Level of approximation	Basis set[a]	R_e (a.u.)	ω_e (cm^{-1})	D_e (eV)
E_0	DZP	3.16	811	0.98
$E_0+E^I_{CORR}$	DZP/MB1	3.12	871	1.37
	DZP/MB2	3.11	878	1.47
	DZP/MB3	—	—	2.04
	DZP/MB4	—	—	2.08
	DZP/MB5	3.07	922	2.08
$E_0+E^I_{CORR}+E_E$	DZP/MB5	3.02	952	2.54
Exp.[b]		2.97	853.8	2.80
MCSCF/CI[c]	[13*s*7*p*5*d*(Cl)/11*s*6*p*5*d*(O)]	—	957[c]	2.69[c]

[a] See comments in the text.
[b] Ref. [3]; $D_e = D_0 + \omega_e/2$.
[c] Slater basis set, Ref. [10]

The zeroth-order wavefunction corresponding to this process, is the following multiconfigurational wavefunction:

$$\Psi_0(\mathrm{ClO}; X^2\Pi) = 1\sigma^2 2\sigma^2(c_1 3\sigma^2 + c_2 3\sigma 4\sigma + c_3 4\sigma^2)1\pi^4 2\pi^3. \tag{13}$$

Once again we have the typical three term expansion extensively discussed previously [1, 2]. Under the rotation (4), this wave-function behaves very similarly to (8) i.e. does not have a diagonal representation.

3.2. Molecular parameters for ClO

The results of Table 7 show the importance of the optimization of the 3*d* correlation orbital on Cl at the E^I_{CORR} level of calculation. Basis sets MB1 to MB5 (details are given in *I*) correspond to the following 3*d* orbitals: atomic SCF orbital (MB2), polarization function (MB3), one-primitive correlation orbital (MB4) and two-primitives correlation orbital (MB5). MB1 does not contain any 3*d* function. The consequence of this optimization i.e. a progressive deepening of the potential well, is a drastic improvement of the dissociation energy value, as illustrated in Fig. 1. The R_e value is also significantly improved but the vibrational frequency is finally overestimated.

Finally, the total energy results ($E_0+E^I_{CORR}+E_E$) are in good agreement with the corresponding experimental results. Discrepancies of respectively 2%, 11% and 9% for R_e, ω_e and D_e are found.

4. The NCl radical

4.1. Zeroth-order wavefunction for the $X^3\Sigma^-$ state

The dissociation process:

$$\mathrm{NCl}(X^3\Sigma^-) \rightarrow \mathrm{N}(^4S) + \mathrm{Cl}(^2P) \tag{14}$$

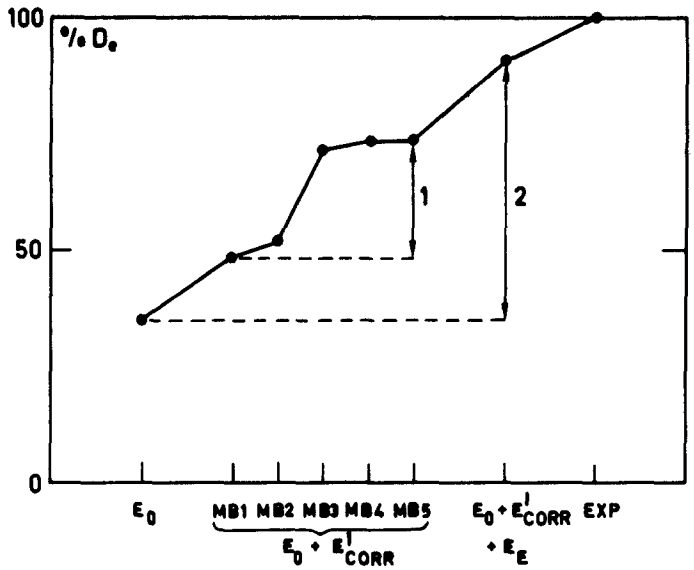

Fig. 1. Correlation and basis set effect on the calculated dissociation energy of the ClO radical. 1) basis set effect on E^1_{CORR}, 2) whole correlation effect

is very similar to that of ClO and hence the corresponding zeroth-order wavefunction is the usual three-SAAP's multiconfiguration function

$$\Psi_0(\mathrm{NCl};\, X^3\Sigma^-) = 1\sigma^2 2\sigma^2(c_1 3\sigma^2 + c_2 3\sigma 4\sigma + c_3 4\sigma^2)1\pi^4 2\pi^2 \tag{15}$$

that cannot be reduced to diagonal form because of the presence of spin recoupling terms as previously discussed in section 2.

4.2. Molecular parameters for the $X^3\Sigma^-$ state

The results of the calculations presented in Table 8 show the decisive improvement of the calculated R_e and ω_e values obtained by the inclusion of the correlation energy. The corresponding total energy results are in good agreement with elaborate MRD-CI calculations on the one hand (0.7% and 5.6% for R_e and ω_e respectively) and with the experimental values on the other hand (2.3% and 5.6% for R_e and ω_e respectively). This agreement is similar to that usually observed for the other calculations presented in this paper so that we think that the value of 2.14 eV which we propose for the dissociation energy should be a lower bound of the exact value with an accuracy of a few tenths of an eV.

4.3. Zeroth-order wavefunctions for the $a^1\Delta$ and $b^1\Sigma^+$ states

The zeroth-order wavefunction corresponding to the dissociation processes:

$$\mathrm{NCl}(a^1\Delta) \rightarrow \mathrm{N}(^2D) + \mathrm{Cl}(^2P) \tag{16}$$

$$\mathrm{NCl}(b^1\Sigma^+) \rightarrow \mathrm{N}(^2D) + \mathrm{Cl}(^2P) \tag{17}$$

Table 8. Molecular parameters for NCl

Level of approximation	Basis[a] set	$X^3\Sigma^-$			$a^1\Delta$				$b^1\Sigma^+$			
		R_e (a.u.)	ω_e (cm^{-1})	D_e (eV)	R_e (a.u.)	ω_e (cm^{-1})	D_e (eV)	T_e (eV)	R_e (a.u.)	ω_e (cm^{-1})	D_e (eV)	T_e (eV)
E_0	DZP	3.29	646	1.15	3.17	700	2.19	1.85	3.0	938	0.84	3.21
$E_0+E^I_{CORR}$	DZP/MB5	3.18	758	1.77	3.10	831	3.03	1.63	3.08	936	2.42	2.26
$E_0+E^I_{CORR}+E_E$	DZP/MB5	3.12	781	2.14	3.06	878	3.28	1.29	3.05	1020	2.47	2.10
Exp.		3.051[b]	827[b]			904[c]		1.15[c]	2.969[b]	935.6[b]		1.857[b]
MRD-CI[c]		3.099	827		3.02	940		1.36	2.969	936		2.18

[a] See comments in the text.
[b] Ref. [3].
[c] Ref. [6]

Table 9. Zeroth-order wavefunction for NCl $b^1\Sigma^+$

Occupation numbers of the catesian SAAP's								Predominance along the dissociation path		Symbolic weight
								$^1\Delta$	$^1\Sigma^+$	$^1\Sigma^+$
1σ	2σ	3σ	4σ	$1\pi_x$	$2\pi_x$	$1\pi_y$	$2\pi_y$			
2	2	2	0	2	2	2	0	equilibrium and dissociation $N(^2D_{\pm 2})+Cl(^2P_0)$	equilibrium [a]	*a*
2	2	2	0	2	0	2	2			*b*
2	2	0	2	2	2	2	0			*c*
2	2	0	2	2	0	2	2			*d*
2	2	2	2	1	1	2	0			*e*
2	2	2	2	2	0	1	1	dissociation $N(^2D_{\pm 1})+Cl(^2P_{\pm 1})$	dissociation $N(^2D_{\pm 1})+Cl(^2P_{\mp 1})$	*f*
2	2	2	0	1	1	2	2			*g*
2	2	2	0	2	2	1	1			*h*

[a] These two SAAP's are added so that the same set of SAAP's describes both dissociation processes

are presented in their cartesian form in the first column of Table 9. Providing we use a diagonal representation of the SAAP's corresponding to the $N(^2D_{\pm 2})+Cl(^2P_0)$ coupling of the $^1\Delta$ channel, it is the same set of SAAP's that describe both processes[2] so that the $^1\Delta$ and $^1\Sigma^+$ states will correspond respectively to the first and second root of the MCSCF or CI calculations. In the second column of this table we roughly describe the R values where the different SAAP's have a predominant weight, and we finally indicate in the last column a label for those SAAP's.

4.4. Molecular parameters for the $a^1\Delta$ and $b^1\Sigma^+$ states

The total energy results for the parameters R_e, ω_e and T_e of the $^1\Delta$ state are in good agreement with MRD-CI calculations on the one hand and with the available experimental results on the other hand with discrepancies of 0.3%, 3%, 12% respectively. The electronic term T_e of the $^1\Sigma^+$ state is also decisively improved (60%) by the inclusion of the correlation energy. This reduction of the calculated value of the terms of both $^1\Delta$ and $^1\Sigma^+$ states with the inclusion of the correlation energy was forseeable due to the fact that singlet states have more correlation energy than the triplet states as a consequence of the exclusion principle. On the contrary, the calculated R_e and ω_e values for this state are not improved by the inclusion of the correlation energy; this is particularly true for ω_e for which the agreement with the experimental value goes from 0.2% to 9% when taking the correlation energy into consideration; in view of the other results, however, the former agreement is obviously fortuitous.

[2] In fact the SAAP's labelled *c* and *d* are not necessary to describe the dissociation process of the $^1\Sigma^+$ state; they are simply added so that the same set of SAAP's can be used in the calculation of the $^1\Delta$ and $^1\Sigma^+$ states. It will be shown below that their weights in the MC calculations are always small

Finally, our results predict values of 3.28 eV and 2.47 eV for the dissociation energies of the $^1\Delta$ and $^1\Sigma^+$ states. These values should have roughly the same accuracy as that found for the $^3\Sigma^-$ state.

4.5. Potential energy curves for the $b^1\Sigma^+$ state

We first present in Fig. 2 three MCSCF calculations performed with the extended (DZP) basis set. The curve labelled 1 corresponds to an MCSCF calculation including the SAAP's *a* to *h* discussed in the previous section. This curve results from an avoided crossing between two sets of SAAP's. The first one (curve 2) is composed of the SAAP's *a* and *b* describing the molecule near its equilibrium geometry (plus the SAAP's *c* and *d* the importance of which was discussed before); at large internuclear separation, this set correlates to the incorrect dissociation products $N(^2P)+Cl(^2P)$. The second one (curve 3) involves the SAAP's *e* to *h* describing the correct Wigner-Witmer dissociation products $N(^2D)+Cl(^2P)$. Due to the lack of configurations predominant at intermediate internuclear separations, in the complete zeroth-order wavefunction (SAAP's *a* to *h*), the change between the first and the second set of SAAP's occurs very

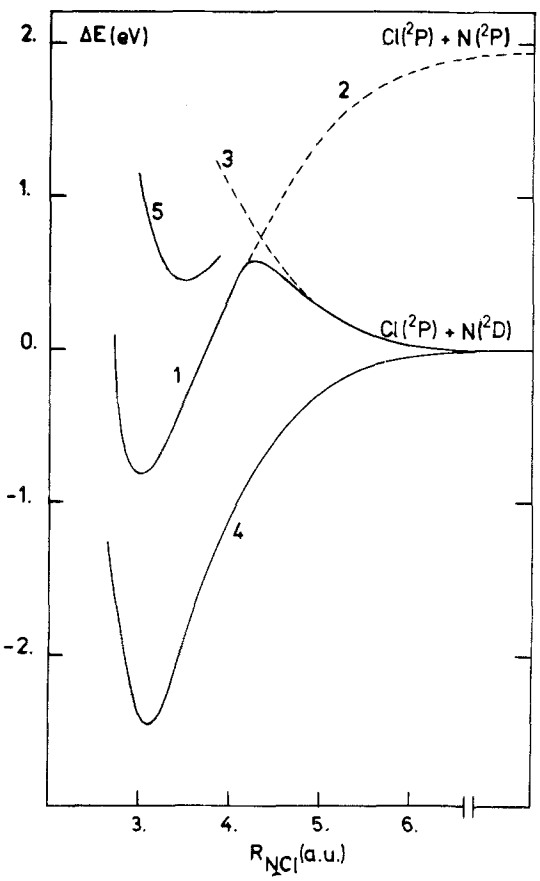

Fig. 2. Potential energy curves for the $b^1\Sigma^+$ state of the NCl radical. The levels of approximation are: 1) $MC_0(DZP)$ with SAAP's *a* to *h*, 2) $MC_0(DZP)$ with SAAP's *a* to *d*, 3) $MC_0(DZP)$ with SAAP's *e* to *h*, 4) Total energy $(E_0+E^1_{CORR}+E_E)$ (this curve is normalized at $R\to\infty$ with the $MC_0(DZP)$ curve), 5) $MC_0(MB5)$ with SAAP's *a* to *h*

Table 10. MCSCF coefficients of the zeroth-order wavefunction corresponding to the dissociation of the $b^1\Sigma^+$ state of NCl

SAAP[a]	R_{NCl}(a.u.)	3.8	4.0	4.2	4.4	4.5	4.6	4.8	5	5.2
a		.681994	.675970	.154968	.110277	.648829	.079276	−.059916	−.042286	−.031106
b		.686189	.676688	.153865	.110814	.648708	.080926	−.056543	−.044056	−.033145
c		−.176191	−.205627	−.015522	−.011137	−.280778	−.008468	.006743	.005134	.004096
d		−.175746	−.205628	−.015415	−.011186	−.280743	−.008612	.006476	.005269	.004203
e		−.001829	.003135	.195144	.256397	.012138	.314861	−.353387	−.406390	−.433380
f		.005372	.004802	.197003	.255239	.012120	.309737	−.368366	−.390600	−.420656
g		.020787	−.011116	−.658594	−.651190	−.011294	−.634405	.592270	.593874	.571584
h		−.040421	−.020896	−.664225	−.648364	−.11117	−.624081	.617872	.570797	.553554
	E_0(DZP)(a.u.)	−24.1737	−24.1629	−24.1573	−24.1599	−24.1405	−24.1632	−24.1666	−24.1698	−24.1724

[a] See Table 9

abruptly and as a consequence, an important maximum (~0.6 eV) occurs in the potential curve 1. In order to illustrate more quantitatively the change taking place in the composition of the zeroth-order wavefunction, we give in table 10 the MCSCF mixing coefficients in the vicinity of the crossing. As the internuclear separation changes from 4.0 to 4.2 a.u., there is a spectacular change in the weights of the SAAP's a, b, g and h; it is this change which is responsible for the potential maximum.

When the remaining correlation energy is introduced (curve 4)[3] the hump disappears completely and the resulting dissociation curve is very smooth; the complete calculation of the correlation energy hence corrects the deficiency of the zeroth-order wavefunction (curve 1). We also present in Fig. 2 a calculation performed with the minimal basis set MB5 (curve 5) showing the metastability (~0.5 eV) of the $^1\Sigma^+$ state when this basis set is used.

5. Conclusion

In this work we have shown that our simplified method for molecular correlation energy calculations can be applied to molecules containing third row atoms providing some methodological developments are made as described in the first paper of this series. The calculated results presented here for some diatomic chlorinated species are found in good agreement with the corresponding experimental and/or large scale CI values. We have considered properties that are very sensitive to correlation effects, as illustrated in Fig. 3. This figure shows the spectacular improvement of the results (energy differences ΔE (T_e and D_e) and R_e) with the progressive inclusion of the correlation energy; however, a more erratic dependence is observed for ω_e values.

The figure represents the fraction of the total energy results (in percent) obtained at the successive steps of the energy calculations. The following conclusions can be drawn:

i) Correlation effects increase D_e and ω_e values and decrease T_e and R_e values.

ii) The inclusion of the internal correlation energy considerably reduces the dispersion of the results.

iii) The calculated results exhibit discrepancies of about 10% for ΔE and ω_e and 2% for R_e with respect to the corresponding experimental values.

Let us remark that the present methodology maintains the economical features that were pointed out previously for systems including only second row atoms i.e. small size (2 to 8 SAAP's) extended basis set MCSCF calculations and limited size CI calculations performed with minimal basis sets. However, our results compare very well (excepting vibrational frequencies) with other calculated values proceeding from elaborate MCSCF, MCSCF-CI, SCEP/CEPA, PNO/CEPA, CEPA, PNO-CI and POL-CI calculations mostly performed with very large

[3] This curve is normalized to coincide with the MC_0 curve at infinite internuclear separation

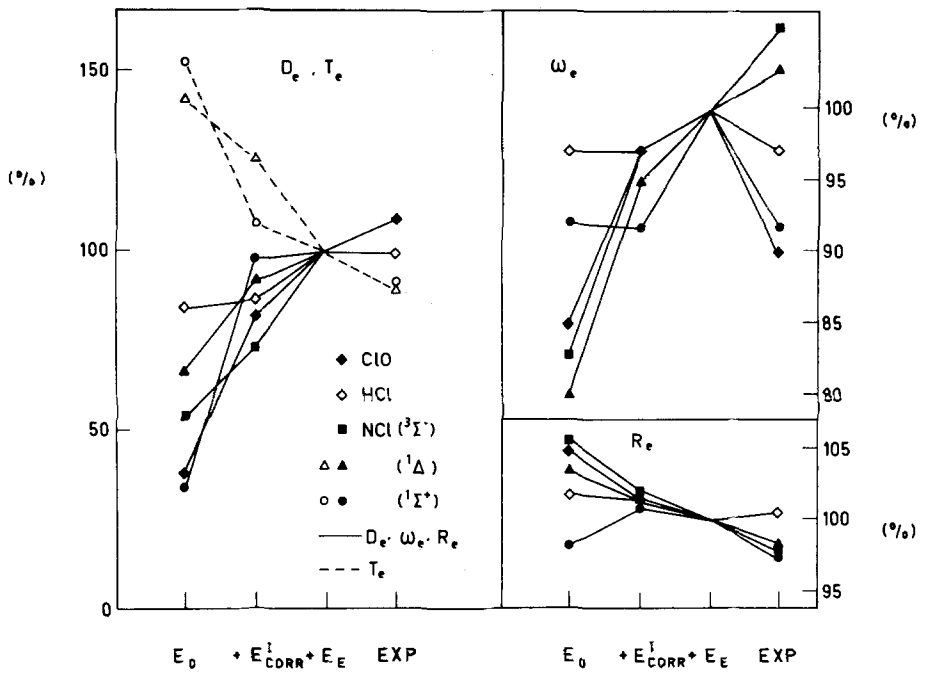

Fig. 3. Correlation effect on the calculated D_e, T_e, R_e and ω_e molecular parameters of the HCl, ClO and NCl molecules. The fraction (in percent) of the calculated value is indicated for each step of the calculation, as the available experimental data. The results are normalized to the $E_0 + E^I_{CORR} + E_E$ level in order to point out the agreement between the total energy and the experimental values

Gaussian and Slater basis sets (see footnotes of Tables 2 to 8 for more details).

The pursuit of this work, limited up till now to chlorinated molecules, will be on the one hand the study of larger polyatomic systems and on the other hand the consideration of other third-row atoms of chemical importance.

Acknowledgments. The authors thank Prof. G. Verhaegen for critical discussions and comments about the manuscript. They are also grateful to the "Ministère de la Politique Scientifique" for a "Action de Recherche Concertée" (ARC) and to the "Fonds de la Recherche Fondamentale Collective" (FRFC) for a research contract.

References

1. Lievin, J., Breulet, J., Clercq, Ph., Metz, J.-Y.: Theoret. Chim. Acta (Berl.) **61**, 513 (1982)
2. Metz, J.-Y., Lievin, J.: Theoret. Chim. Acta (Berl.) **62**, 195 (1983)
3. Huber, K. P., Herzberg, G.: Molecular Spectra and Molecular Structure IV. Constants of diatomic molecules. New York: Van Nostrand Reinhold 1979
4. Sheasley, W. D., Mathews, C. W.: J. Mol. Spectr. **47**, 420 (1973)
5. Rosmus, P., Meyer, W.: J. Chem. Phys. **66**, 13 (1977)
6. Bettendorff, M.: "XVIe Congrès des Chimistes Théoriciens d'Expression Latine" Louvain-la-Neuve (Belgium) (1983)

7. Werner, H. J., Rosmus, P.: J. Chem. Phys. **73**, 2319 (1980)
8. Hay, P. J., Wadt, W. R., Kahn, L. R.: J. Chem. Phys. **68**, 3059 (1978)
9. Rosmus, P., Meyer, W.: J. Chem. Phys. **66**, 13 (1977)
10. Arnold, J. O., Whiting, E. E., Langhoff, S. R.: J. Chem. Phys., **66**, 4459 (1977)
11. Lie, G. C., Clementi, E.: J. Chem. Phys. **60**, 1275 (1974)
12. Meyer, W., Rosmus, P.: J. Chem. Phys. **63**, 2356 (1975)
13. Bettendorff, M., Buenker, R. J., Peyerimhoff, S. D., Römelt, J.: Z. Phys. A **304**, 125 (1982)

Received April 13, 1984/September 14, 1984